CDDpress

www.nature.com/cdd

ARTICLE

A viral interferon regulatory factor degrades RNA-binding protein hnRNP Q1 to enhance aerobic glycolysis via recruiting E3 ubiquitin ligase KLHL3 and decaying GDPD1 mRNA

Xiaoyu Qi[1,2,3,5], Qin Yan[1,2,3,5], Yuancui Shang[2], Runran Zhao[2], Xiangya Ding[1], Shou-Jiang Gao[4], Wan Li[1,2,3]✉ and Chun Lu[1,2,3]✉

Reprogramming of host metabolism is a common strategy of viral evasion of host cells, and is essential for successful viral infection and induction of cancer in the context cancer viruses. Kaposi's sarcoma (KS) is the most common AIDS-associated cancer caused by KS-associated herpesvirus (KSHV) infection. KSHV-encoded viral interferon regulatory factor 1 (vIRF1) regulates multiple signaling pathways and plays an important role in KSHV infection and oncogenesis. However, the role of vIRF1 in KSHV-induced metabolic reprogramming remains elusive. Here we show that vIRF1 increases glucose uptake, ATP production and lactate secretion by downregulating heterogeneous nuclear ribonuclear protein Q1 (hnRNP Q1). Mechanistically, vIRF1 upregulates and recruits E3 ubiquitin ligase Kelch-like 3 (KLHL3) to degrade hnRNP Q1 through a ubiquitin–proteasome pathway. Furthermore, hnRNP Q1 binds to and stabilizes the mRNA of glycerophosphodiester phosphodiesterase domain containing 1 (GDPD1). However, vIRF1 targets hnRNP Q1 for degradation, which destabilizes GDPD1 mRNA, resulting in induction of aerobic glycolysis. These results reveal a novel role of vIRF1 in KSHV metabolic reprogramming, and identifying a potential therapeutic target for KSHV infection and KSHV-induced cancers.

Cell Death & Differentiation (2022) 29:2233–2246; https://doi.org/10.1038/s41418-022-01011-1

INTRODUCTION

According to the assessment of the International Agency for Research on Cancer, viral infection accounts for approximately 12% of human cancer worldwide [1]. Kaposi's sarcoma-associated herpesvirus (KSHV), identified in an AIDS-associated Kaposi's sarcoma (AIDS-KS) lesion [2], is one of the seven human oncogenic viruses and the causative agent of Kaposi's sarcoma (KS), primary effusion lymphoma (PEL), multicentric Castleman's diseases (MCD), and KSHV-associated inflammatory cytokine syndrome (KICS) [3, 4]. Despite decades of studies, the precise mechanism of KSHV infection and induction of tumors is still unclear.

All cells require energy in the form of adenosine triphosphate (ATP) to sustain life activities including proliferation and response to environmental stress. For normal cells, glucose is the major carbon source, which is metabolized to carbon dioxide via glycolysis, tricarboxylic acid (TCA) cycle and oxidative phosphorylation to produce ATP under an aerobic condition. In this case, minimal amount of lactate is produced. A large amount of lactate is only produced under anaerobic conditions. In contrast, cancer cells reprogram the glycolytic pathway and shunt the carbon from glucose to lactate even in the presence of adequate oxygen supply [5–7]. This metabolic process is termed aerobic glycolysis, also known as the Warburg Effect. The common feature of aerobic glycolysis is increased glucose uptake and decreased mitochondrial oxidative phosphorylation. Aerobic glycolysis is essential for supporting the anabolic proliferation and energetic requirements of a variety of cancers, and therefore has been regarded as a core hallmark of cancer [8]. Numerous viruses have also been shown to reprogram metabolic pathways and enhance aerobic glycolysis [9–16].

The KSHV life cycle comprises two phases, including the latent and lytic phases. During latency, KSHV only expresses a few genes including LANA (ORF73), vCyclin (ORF72) and vFLIP (ORF71) together with 25 micro-RNAs (miRNAs) derived from a cluster of 12 precursor miRNAs (pre-miRNAs) [17]. By contrast, during lytic replication, KSHV expresses cascades of lytic genes among which replication and transcriptional activator (RTA) encoded by ORF50 is essential and sufficient for initiating KSHV lytic replication [17]. KSHV primary infection and untransformed latent infection switch host cell metabolism from oxidative phosphorylation to aerobic glycolysis [18, 19]. During latent KSHV infection, glucose uptake and lactic acid production are increased and oxygen consumption is significantly reduced [18]. Inhibitors of glycolysis induce apoptosis of KSHV-infected endothelial cells [18], indicating that glycolysis is required for the survival of KSHV-infected endothelial cells. Hypoxia inducible

[1]State Key Laboratory of Reproductive Medicine, Department of Gynecology, Women's Hospital of Nanjing Medical University, Nanjing Maternity and Child Health Care Hospital, Nanjing Medical University, Nanjing 210004, P. R. China. [2]Department of Microbiology, Nanjing Medical University, Nanjing 211166, P. R. China. [3]Key Laboratory of Pathogen Biology of Jiangsu Province, Nanjing Medical University, Nanjing 211166, P. R. China. [4]Tumor Virology Program, UPMC Hillman Cancer Center, and Department of Microbiology and Molecular Genetics, University of Pittsburgh, Pittsburgh, PA 15232, USA. [5]These authors contributed equally: Xiaoyu Qi, Qin Yan. ✉email: wanli@njmu.edu.cn; clu@njmu.edu.cn

Edited by V. D'Angiolella

Received: 27 October 2021 Revised: 19 April 2022 Accepted: 20 April 2022
Published online: 10 May 2022

factor (HIF) has been shown to be involved in KSHV-induced aerobic glycolysis in untransformed cells [20]. KSHV microRNAs expressed during latency also function to regulate host cell energy metabolism. Their expression decreases oxygen consumption, increases lactate secretion and glucose uptake in noncancer cells [21], which is important for maintenance of latency during KSHV infection and provides a growth advantage. Meanwhile, KSHV lytic protein K5 potentially contributes to cell proliferation through induction of aerobic glycolysis [22]. Both latent genes, such as LANA and viral miRNAs, and lytic genes including vGPCR and K5, have the potential to regulate the aerobic glycolysis pathway in KSHV-infected endothelial cells and monocytes [20–23]. In contrast, in KSHV-transformed cells, KSHV reduces aerobic glycolysis, TCA cycle and oxidative phosphorylation by activating the NF-κB pathway to inhibit the expression of glucose transporters and glucose uptake [24]. KSHV reprogramming of this metabolic pathway results in reduced oxidative stress and autophagy cell arrest, particularly in nutrient deficiency condition [24]. As a result, KSHV-transformed cells depend on increased glutamine uptake to sustain the requirements for energy and macromolecule building blocks for anabolic proliferation [25, 26]. Despite these studies, how KSHV reprograms the metabolic programs under different replication phases and cell states remain largely unknown [27].

vIRF1 is a 449-amino-acid protein, encoded by KSHV lytic gene ORF-K9 [28]. As a lytic and oncogenic protein, vIRF1 might play an important role in KSHV infection and KS pathogenesis. For instance, overexpression of vIRF1 alone was sufficient to transform mouse embryonic fibroblasts (NIH3T3) cells, and inhibited type I interferon signaling and apoptosis by restraining TGF-beta/Smad signaling and reducing p53 function [29–34]. Our group has recently shown that vIRF1 promotes cell proliferation, invasion, angiogenesis, and cellular transformation in vitro and in vivo [35–38]. However, the role of vIRF1 in KSHV infection and the underlying mechanism of vIRF1-mediated tumorigenesis are still not fully understood. Particularly, the role of vIRF1 in KSHV-induced metabolic reprogramming has not been investigated.

Heterogeneous ribonucleoprotein Q, isoform 1 (hnRNP Q1), is a ubiquitous mRNA binding protein [39, 40], also called synaptotagmin binding cytoplasmic RNA interacting protein (SYNCRIP) [39]. hnRNP Q1 is a member of the cellular hnRNP family and contains two different RNA-binding domains, three RNA recognition motifs in the central region, and a single arginine- and glycine-rich region (RGG box) at the C-terminus for binding to RNA [41]. It is associated with the motor neurons (SMN) complex [41], and has a wide range of functions in multiple aspects of mRNA biogenesis and functions including maturation, nuclear export, translation, stability, splicing, and editing [1, 42–45]. hnRNP Q1 is mainly localized to the cytoplasm, which is distinct from other hnRNP Q isoforms expressed in the nucleus supporting the notion that hnRNP Q1 might play an important role in regulating mRNA localization, translation and stability [41]. Indeed, hnRNP Q1 has been reported to regulate Cdc42 mRNA localization [46], inhibit Gap-43 mRNA translation [46], and control c-myc mRNA stability [45].

In the present work, we sought to investigate the role of vIRF1 in KSHV regulation of cellular metabolism. We observed that vIRF1 induced aerobic glycolysis by inhibiting hnRNP Q1 expression. Mechanistically, vIRF1 recruited E3 ubiquitin ligase Kelch-like 3 (KLHL3) to degrade hnRNP Q1. Furthermore, the interaction between hnRNP Q1 and the mRNA of glycerophosphodiester phosphodiesterase domain containing 1 (GDPD1) promoted the stability of GDPD1 mRNA, resulting in decrease of GDPD1 protein level, which contributed to vIRF1-induced aerobic glycolysis. Our findings indicate that vIRF1 functions as a regulator of aerobic glycolysis and hence providing insights into the molecular basis of KSHV infection and KSHV-induced oncogenesis.

RESULTS

vIRF1 downregulates hnRNP Q1 to promote aerobic glycolysis

Although hnRNP Q1, an RNA-binding protein, has been implicated in tumorigenesis [47, 48], its role in KSHV infection and KS pathogenesis remains unknown. In mass spectrometry analysis [35, 38], hnRNP Q1 is down-regulated by 1.56-fold in vIRF1-transduced cells. We transduced endothelial cell line EA.hy926 with lentiviral vIRF1 at a MOI of 2 as previously described [35] and observed a decrease of hnRNP Q1 in vIRF1-transduced cells (Fig. 1A). KSHV infection of EA.hy926 cells also reduced hnRNP Q1 expression (Fig. 1B). Most importantly, we observed downregulation of hnRNP Q1 protein in KS lesions compared to normal skin tissues (Fig. 1C, D).

Metabolic reprograming is essential for KSHV infection and KSHV-induced cellular transformation [27, 49]. However, whether vIRF1 regulates metabolic pathways remains unknown. We examined glucose uptake, ATP production and lactate production in vIRF1 overexpressed cells. An increase of glucose uptake in vIRF1 transduced cells was observed (Fig. 2A). vIRF1-transduced cells also had higher levels of intracellular ATP and produced more lactate (Figs. 2B and 2C). Hexokinase 2 (HK2) is often a rate-limiting enzyme for the metabolism of glucose while glucose transporter 1 (GLUT1) and GLUT3 are responsible for increased glucose uptake. We found that overexpression of vIRF1 strongly increased the protein levels of HK2, GLUT1 and GLUT3 (Fig. 2D).

To determine whether downregulation of hnRNP Q1 regulated vIRF1-induced aerobic glycolysis, we transduced hnRNP Q1 in vIRF1-expressing cells and found that overexpression of hnRNP Q1 not only reduced protein levels of HK2, GLUT1 and GLUT3 (Fig. 2E), but also decreased levels of glucose uptake, ATP production and lactate production (Fig. 2F–H). In contrast, knockdown of hnRNP Q1 by using short hairpin RNAs (shRNAs) targeting hnRNP Q1 increased the protein levels of HK2, GLUT1 and GLUT3, and the levels of glucose uptake, ATP production and lactate secretion (Fig. 2I–L; Fig S1). These data suggest that vIRF1 promotes aerobic glycolysis via downregulation of hnRNP Q1.

vIRF1 induces hnRNP Q1 degradation

To examine the mechanism by which vIRF1 negatively regulated hnRNP Q1, we performed co-immunoprecipitation assay. We found that vIRF1 interacted with hnRNP Q1 (Fig. 3A–C; Fig S2). GST pull-down assay showed that GST-vIRF1 but not the GST control was associated with His-hnRNP Q1 (Fig. 3D). Immunofluorescence staining assay (IFA) showed that vIRF1-Flag not only reduced the hnRNP Q1-Myc expression level in endothelial cells (Fig. 3E), but also exhibited colocalization with hnRNP Q1-Myc (Fig. 3F).

Quantitative reverse transcription PCR (qRT-PCR) showed that neither vIRF1 transduction nor KHSV infection affect the mRNA level of hnRNP Q1 (Figs. 4A, B). Therefore, we further examined whether vIRF1 regulated hnRNP Q1 protein stability. We treated the cells with cycloheximide (CHX) and found that vIRF1 promoted hnRNP Q1 degradation (Fig. 4C, D). Furthermore, treatment with MG132 effectively blocked vIRF1-mediated hnRNP Q1 reduction (Fig. 4E, F). Consistent with these observations, hnRNP Q1 underwent marked polyubiquitylation in the presence of MG132 in vIRF1-expressing cells (Fig. 4G), as well as in KSHV-infected cells (Fig S3), indicating that vIRF1 induced hnRNP Q1 degradation via the proteasome-dependent pathway. Moreover, more K48-ubiquitinated hnRNP Q1 was detected in vIRF1-transduced cells than the control cells (Fig. 4H).

There are 34 lysine (K) residues distributed in the four domains of hnRNP Q1 (AcD, RRM1, RRM2, and RRM3). To identify the major ubiquitination site(s) in hnRNP Q1 protein, we mutated all lysine (K) sites by replacing a lysine (K) with an arginine (R) in each domain to generate hnRNP Q1 mutants, named MD1, MD2, MD3 and MD4, respectively (Fig. 4I), and examined the effect of vIRF1 on their expression and ubiquitination. Mutations of all Ks in RRM3 domain of hnRNP Q1 (hnRNP Q1_MD4 mutant) reversed

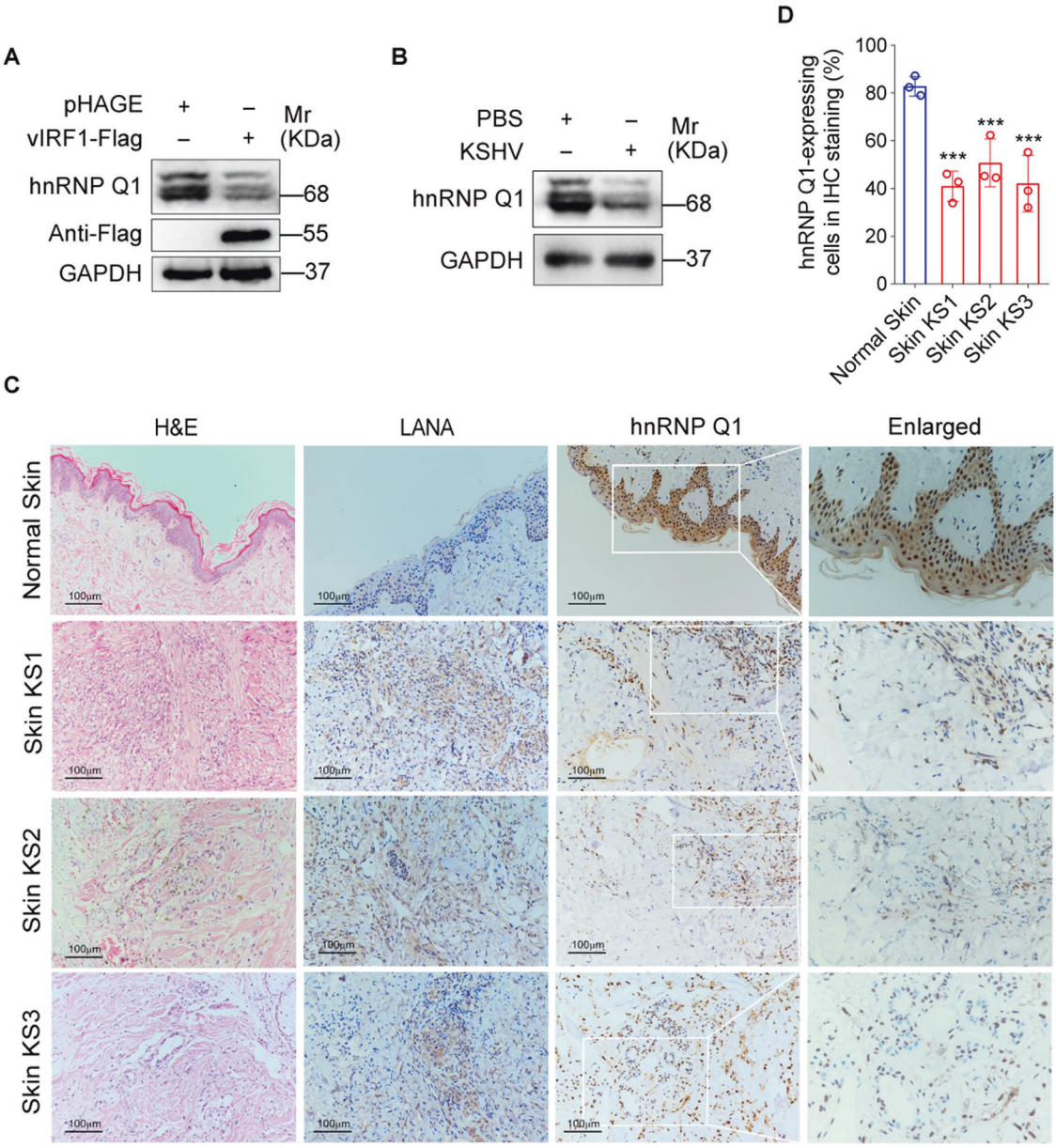

Fig. 1 vIRF1 downregulates hnRNP Q1. A A human umbilical vein endothelial cell line EA.hy926 were transduced with 2 MOI lentiviral vIRF1 (**vIRF1**) or control lentivirus (**pHAGE**). Whole-cell lysates were collected and examined by Western blotting for hnRNP Q1 expression. **B** Endothelial cells EA.hy926 were treated with PBS (**PBS**) or infected with wild type KSHV (**KSHV**). Whole-cell lysates were collected and examined by Western blotting for hnRNP Q1 expression. **C** H&E staining, immunohistochemical staining of KSHV LANA, hnRNP Q1 in normal skin, skin KS of patient #1 (**Skin KS1**), skin KS of patient #2 (**Skin KS2**), and skin KS of patient #3 (**Skin KS3**). Magnification, ×200, ×400. **D** Results were quantified in **C** Data were presented with mean ± SD. ***$P < 0.001$, Student's *t*-test.

the inhibition of hnRNP Q1 expression caused by vIRF1 (Fig. 4J). We further mutated each K site in hnRNP Q1 RRM3 domain and found that mutation of K363 (hnRNP Q1_363KR) alone was sufficient to abolish the degradation of hnRNP Q1 induced by vIRF1 (Fig. 4K). Consistently, hnRNP Q1_363KR ubiquitination was attenuated compared with that of wild type hnRNP Q1 (Fig. 4L). Taken together, these data suggest that K363 is a critical residue of hnRNP Q1 involved in vIRF1-mediated hnRNP Q1 ubiquitination.

vIRF1 recruits the E3 ubiquitin ligase KLHL3 to degrade hnRNP Q1

Since E3 ubiquitin ligase kelch like family member 3 (KLHL3) interacts with hnRNP Q1 [39], we hypothesized that vIRF1 might recruit KLHL3 to ubiquitinate hnRNP Q1. We found a higher expression level of KLHL3 protein in both vIRF1-expressing cells and KSHV-infected cells (Fig. 5A, B). Furthermore, there were more KLHL3-postive cells in KS lesions than normal skin tissues (Fig. 5C, D). Co-immunoprecipitation assay confirmed the interaction of KLHL3 with hnRNP Q1 (Fig. 5E, F). To evaluate the effect of KLHL3 on hnRNP Q1, we overexpressed KLHL3, and found that overexpression of KLHL3 not only dramatically reduced hnRNP Q1 protein expression but also caused an increase of hnRNP Q1 ubiquitination (Fig. 5G, H). As a component of a cullin-RING E3 ubiquitin ligase (CRL) complex, KLHL3 interacted with the CUL3 (cullin 3) to promote substrate ubiquitination [50]. We found that vIRF1 increased the interaction between KLHL3 and CUL3 (Fig. 5J) without significantly affecting CUL3 protein expression (Fig. 5I). Consistent with these observations, KSHV infection also enhanced the interaction of KLHL3 and CUL3 (Fig S4). These data revealed

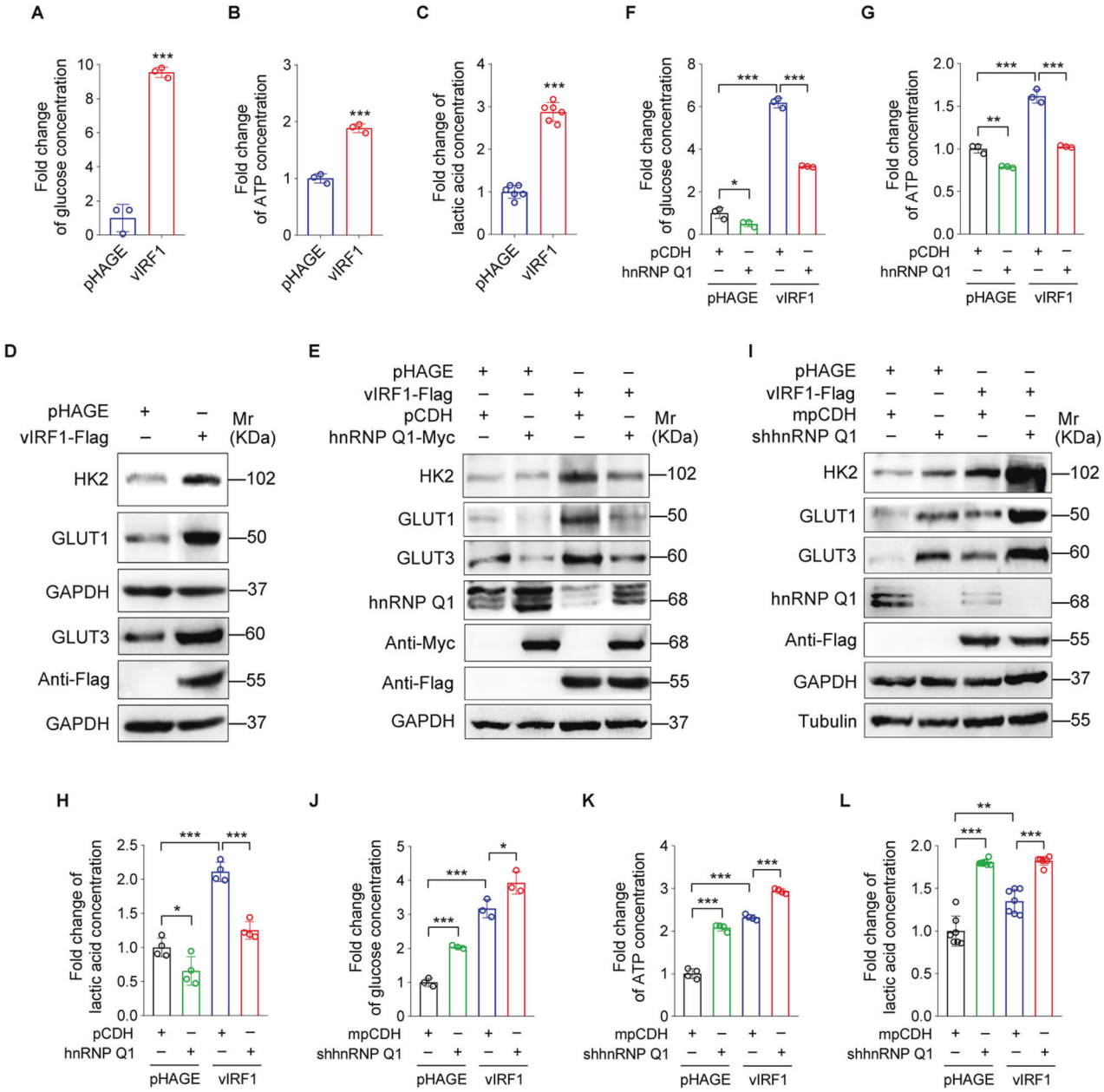

Fig. 2 vIRF1 downregulates hnRNP Q1 to promote aerobic glycolysis. A Levels of intracellular glucose of endothelial cells transduced with 2 MOI lentiviral vIRF1 (**vIRF1**) or control lentivirus (**pHAGE**). **B** Levels of intracellular ATP of cells treated as in (**A**), **C**. The supernatant of cells treated as in (**A**) was used to measure lactate production. **D** Western blotting analysis of HK2, GLUT1, and GLUT3 expression in cells treated as in (**A**). **E** Lentiviral vIRF1- or its control pHAGE-infected endothelial cells were transduced with lentiviral hnRNP Q1 and its control pCDH. Whole-cell lysates were harvested and examined by Western blotting for HK2, GLUT1 and GLUT3 expression. **F** Cells treated as in (**E**) were used to examine the levels of intracellular glucose. **G** Cells treated as in (**E**) were used to measure the levels of intracellular ATP. **H** Cells treated as in (**E**) were used to measure lactate production. **I** Lentiviral vIRF1- or its control pHAGE-infected endothelial cells were transduced with lentivirus expressing a mixture of shRNAs targeting hnRNP Q1 (shhnRNP Q1) and its control mpCDH. Whole-cell lysates were harvested and examined by Western blotting for HK2, GLUT1 and GLUT3 expression. **J** Cells treated as in (**I**) were used to examine the levels of intracellular glucose. **K** Cells treated as in **I** were used to measure the levels of intracellular ATP. (**L**). Cells treated as in (**I**) were used to measure lactate production. Data were presented with mean ± SD. *$P < 0.05$, **$P < 0.01$, and ***$P < 0.001$, Student's *t*-test.

that vIRF1 degraded hnRNP Q1 by facilitating the formation of KLHL3/CUL3 ubiquitin ligase complex.

Next, we asked whether upregulated KLHL3 might affect vIRF1-induced aerobic glycolysis. We transduced vIRF1-expressing cells with shRNAs targeting KLHL3 (shKLHL3) to cause knockdown of KLHL3 expression. Knockdown of KLHL3 upregulated hnRNP Q1 expression (Fig S5), and reduced vIRF1-induced glucose uptake, ATP production and lactate production (Fig. 5K–M). Additionally, knockdown of KLHL3 resulted in a reduction in the protein levels of HK2, GLUT1 and GLUT3 (Fig. 5N).

vIRF1 downregulates hnRNP Q1 to increase the instability of GDPD1 mRNA

As an RNA-binding protein, hnRNP Q1 has multiple functions in mRNA metabolism including stability and translation [44, 45]. To search the mRNA target of hnRNP Q1 participated in vIRF1-

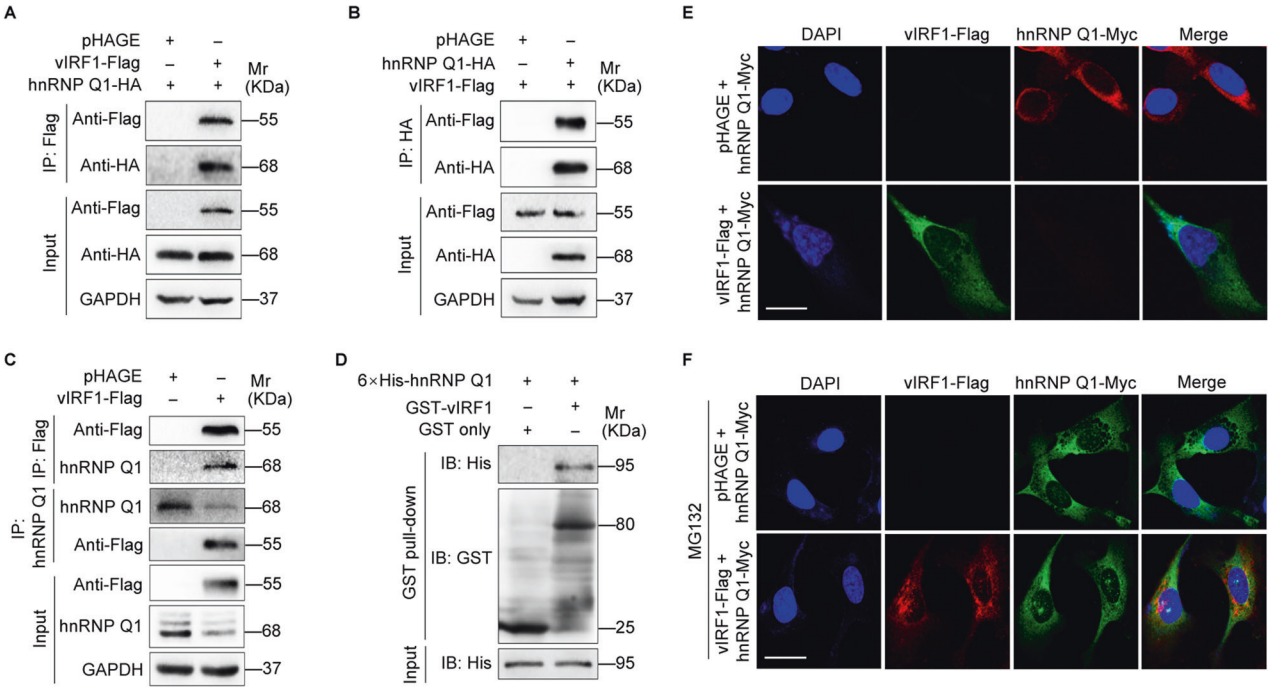

Fig. 3 vIRF1 directly interacts with hnRNP Q1. A Endothelial cells transfected with hnRNP Q1-HA construct were transduced with lentiviral vIRF1-Flag or its control pHAGE. The interaction between vIRF1 and hnRNP Q1 proteins was examined by immunoprecipitating with anti-Flag antibody. **B** Endothelial cells transfected with vIRF1-Flag construct were transduced with lentiviral hnRNP Q1-HA or its control pHAGE. The interaction between vIRF1 and hnRNP Q1 proteins was examined by immunoprecipitating with anti-HA antibody. **C** Lentiviral vIRF1- or its control pHAGE-infected endothelial cells were used to examine the interaction between vIRF1 and hnRNP Q1 proteins by immunoprecipitating with anti-Flag antibody or anti-hnRNP Q1 antibody. **D** GST or GST- vIRF1 fusion protein was used to pull down purified 6 xHis-hnRNP Q1 protein. **E** Endothelial cells transfected with vIRF1-Flag and hnRNP Q1-Myc were employed to detect the expression of vIRF1 and hnRNP Q1 by immunofluorescence staining. **F** Endothelial cells transfected with vIRF1-Flag and hnRNP Q1-Myc were further treated with MG132 (20 μM) for 6 h and then were employed to examine the colocalization of vIRF1 and hnRNP Q1 by immunofluorescence staining.

induced aerobic glycolysis, we firstly analyzed top 15 of the putative hnRNPQ1 of mRNA targets predicted in a previous report [46]. We selected four candidate genes for examination based on potential function in metabolism, unknown role in KSHV infection and KS pathogenesis, and abundant expression in endothelial cells. Of these candidates, qRT-PCR analysis indicated that overexpression of hnRNP Q1 only increased mRNA expression level of glycerophosphodiester phosphodiesterase domain containing 1 (GDPD1) (Fig. 6A). Western blotting showed that overexpression of hnRNP Q1 also upregulated GDPD1 protein level (Fig. 6B). Consistently, knockdown of hnRNP Q1 with shRNAs decreased both the mRNA and protein levels of GDPD1 (Fig. 6C, D). To investigate the association of hnRNP Q1 with GDPD1 mRNA, we performed RNA immunoprecipitation (RIP) followed with qRT-PCR (RIP-qPCR) and confirmed that GDPD1 mRNA was enriched, indicating hnRNP Q1 binding to the GDPD1 mRNA (Fig. 6E). Moreover, both the mRNA and protein levels of GDPD1 was strikingly decreased not only in vIRF1-transduced cells (Fig. 6F, G) but also in KSHV infected cells (Fig. 6H, I). In accordance, there were less GDPD1-positive cells in KS lesions than in normal skin tissues (Fig. 6J, K).

Given that overexpression of hnRNP Q1 in vIRF1-transduced cells dramatically increased GDPD1 mRNA expression level (Fig. 7A), we assumed that the binding of hnRNP Q1 protein to GDPD1 mRNA enhanced its stability. We treated the cells with actinomycin D and performed RNA decay assay. As expected, overexpression of hnRNP Q1 indeed enhanced the stability of GDPD1 mRNA (Fig. 7B). In line with these observations, the stability of GDPD1 mRNA was dramatically reduced by vIRF1 (Fig. 7C).

Next, we explored whether GDPD1 reduction was necessary for vIRF1-induced aerobic glycolysis. Overexpression of GDPD1 significantly inhibited glucose uptake, ATP production and lactate production (Fig. 7D–F), as well as the protein levels of HK2, GLUT1 and GLUT3 (Fig. 7G). Collectively, these data suggest that vIRF1 downregulates hnRNP Q1 to increase the instability of GDPD1 mRNA, resulting in enhancement of aerobic glycolysis.

Loss of vIRF1 reduces KSHV-induced aerobic glycolysis

To further confirm the effect of vIRF1 on aerobic glycolysis, we infected cells with a KSHV mutant virus with deleted ORF-K9 [35] and then transduced these cells with 2 MOI of lentiviral vIRF1 to reconstitute its expression. We found that loss of vIRF1 from the KSHV genome reduced the protein expression level of KLHL3, and increased the expression levels of hnRNP Q1 and GDPD1 proteins (Fig. 8A). Complementation with vIRF1 was sufficient to rescue the expression levels of these proteins (Fig. 8A). We also observed a significant decrease of KLHL3 mRNA and a marked increase of GDPD1 mRNA in the mutant cells compared to both KSHV_wild type infected cells and vIRF1-transduced mutant cells (Fig. 8B). Meanwhile, deletion of ORF K9 lowered KSHV-induced glucose uptake, ATP production, and lactate production, as well as HK2, GLUT1 and GLUT3 expression (Fig. 8C–F), and vIRF1 complementation in cells infected by K9_mut virus completely reversed these effects (Fig. 8C–F).

DISCUSSION

Numerous studies have advanced our understanding of the causes and requirements of aerobic glycolysis in viral infection and cancer [51–53]. Aerobic glycolysis is thought to be an early event in oncogenesis that provides an overall benefit supporting a tumor microenvironment conducive to cancer cell proliferation.

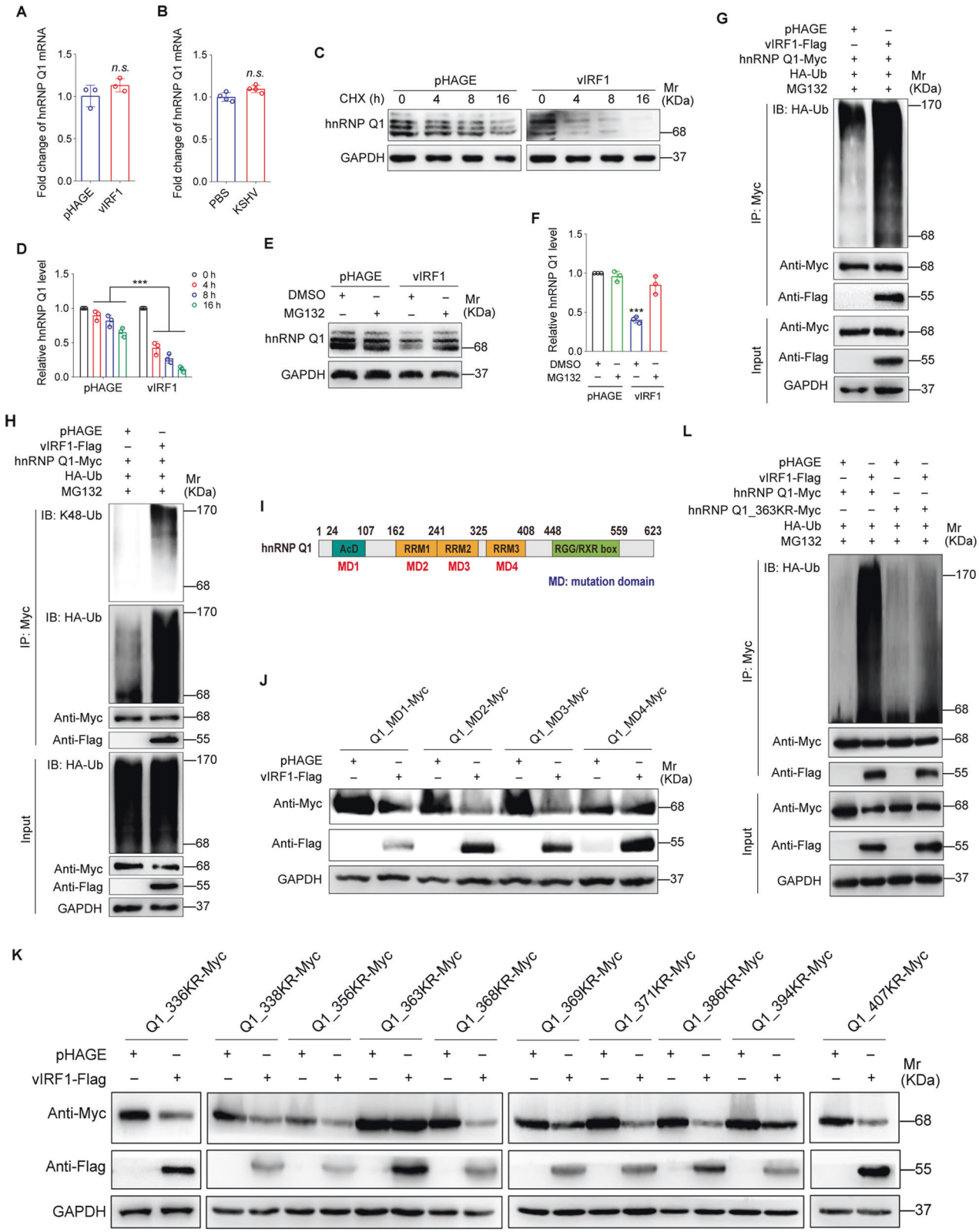

Infections by numerous viruses also induce aerobic glycolysis [11–16]. Accumulating lines of evidence have demonstrated that KSHV infection could induce aerobic glycolysis to support viral replication, as well as the survival and proliferation of untransformed infected cells [18, 20–22, 27, 54], however the mechanisms by which KSHV alters host cell metabolism are poorly understood. In this study, we showed that, in an endothelial cell line, KSHV infection and expression of vIRF1 induce aerobic glycolysis. Specifically, vIRF1 increases glucose uptake, ATP production and lactate secretion. Consistently, loss of vIRF1 from the KSHV genome inhibits KSHV-induced aerobic glycolysis. These findings reveal a novel functional role of vIRF1 in reprogramming of energy

Fig. 4 vIRF1 induces hnRNP Q1 degradation. A qPCR analysis of hnRNP Q1 mRNA expression in endothelial cells transduced with 2 MOI lentiviral vIRF1 (**vIRF1**) or control lentivirus (**pHAGE**). **B** qPCR analysis of hnRNP Q1 mRNA expression in endothelial cells treated with PBS (**PBS**) or infected with wild-type KSHV (**KSHV**). **C** Western blotting analysis of hnRNP Q1 expression in vIRF1-expressing endothelial cells treated with CHX (20 μg/ml) for 0 h, 4 h, 8 h and 16 h. **D** Results were quantified in (**C**). **E** Western blotting analysis of hnRNP Q1 level in vIRF1-expressing endothelial cells treated with MG132 (20 μM) for 6 h (**F**) Results were quantified in (**E**). **G** Endothelial cells treated as in (**A**) were transfected with the HA-Ub and hnRNP Q1-Myc construct, and then treated with MG132 (20 μM) for 6 h. Immunoprecipitation assay was used for detection of hnRNP Q1 ubiquitination with anti-Myc antibody. **H** Cells treated as in (**A**) were treated with MG132 (20 μM) for 6 h. Immunoprecipitation assay was used to detect the level of K48-ubiquitinated hnRNP Q1 with anti-Myc antibody. **I** Schematic representation of hnRNP Q1 with the indicated locations of the AcD and RRM globular domains and the RGG/RXR box motif. **J** Generation of the mutation constructs of hnRNP Q1 in which Lys was replaced with Arg (K to R) based on four domains of hnRNP Q1. Lentiviral vIRF1 or its control pHAGE transduced cells were transfected with plasmids encoding Myc-tagged wild type hnRNP Q1 or its mutation domain constructs (MD1, MD2, MD3 and MD4), respectively. Western blotting was performed to examine hnRNP Q1 expression with anti-Myc antibody. **K** Generation of the mutation constructs of hnRNP Q1 in which Lys was replaced with Arg (K to R) based on mutation domain 4 of hnRNP Q1. Lentiviral vIRF1 or its control pHAGE transduced cells were transfected with plasmids encoding 9 mutation constructs in mutation domain 4 (MD4) of Myc-tagged hnRNP Q1 (336KR, 338KR, 356KR, 363KR, 368KR, 369KR, 371KR, 386KR, 394KR and 407KR), respectively. Western blotting was performed to detect hnRNP Q1 expression level with anti-Myc antibody. **L** Cells treated as in (**A**) were transfected with the HA-Ub and hnRNP Q1-Myc or hnRNP Q1_363KR-Myc construct, and then treated with MG132 (20 μM) for 6 h. Cells were subjected to immunoprecipitation assay (IP) for detection of hnRNP Q1 ubiquitination with anti-Myc antibody. Data were presented with mean ± SD. ***$P < 0.001$, Student's *t*-test. *n.s.*, not significant.

metabolism and highlight new potential avenues to inhibit KSHV infection.

vIRF1 is an early viral lytic gene. Thus, our results indicate that vIRF1 might regulate metabolic pathways during KSHV lytic replication. However, we and other have also demonstrated that vIRF1 is expressed at a low level during viral latency [1, 36], indicating that vIRF1 might have a critical role in regulating cellular metabolism at this stage of KSHV infection. Indeed, the induction of aerobic glycolysis and decrease of oxidative phosphorylation has been observed in latent KSHV infection of endothelial cells, and treatment with inhibitors of aerobic glycolysis could selectively induce apoptosis in KSHV latently infected cells [18], suggesting that aerobic glycolysis is necessary for maintenance of KSHV latently infected cells, and promotes the proliferation of KSHV-infected cells. However, latent KSHV infection of human foreskin fibroblast cells did not induce increased glycolysis or decreased oxygen consumption, and KSHV-infected Burkitt's lymphoma BJAB cells have similar sensitivity to aerobic glycolysis inhibitions with uninfected BJAB cells [18]. In KSHV-transformed primary rat metanephric mesenchymal precursor cells (MM), aerobic glycolysis, TCA cycle and oxidative phosphorylation are reduced by KSHV [24]. In this system, it is glutamine but not glucose that sustains the requirements for energy and essential building blocks for the proliferation of KSHV-transformed cells [25, 26]. It has been reported that mesenchymal cells have high level of aerobic glycolysis [21]. Apparently, inhibition of glucose uptake and aerobic glycolysis prevents KSHV-transformed cells from oxidative stress and autophagy cell arrest [24]. These studies indicate that KSHV-transformed and untransformed cells might use different strategies to regulate the glycolytic pathway, which might depend on the types of cells and stages of KSHV infection [27].

In this study, we infected endothelial cell line EA.hy926 with KSHV and observed the induction of aerobic glycolysis. Increasing evidence shows that both KSHV latent and lytic products impact aerobic glycolysis [21, 54, 55]. Thus, aerobic glycolysis might contribute to multiple processes of KSHV infection and KS pathogenesis. Furthermore, we showed the critical role of vIRF1 in KSHV-induced cell proliferation, invasion, angiogenesis, and cellular transformation in vitro and in vivo [35–38]. Here, we further observed its effect on the induction of aerobic glycolysis, which support its role in regulating aerobic glycolysis during KSHV infection and replication.

Emerging evidence has shown that the increased growth rate of cancer cells is a consequence of glycolytic shift (aerobic glycolysis), prompting a decrease in oxidative phosphorylation and mitochondrial density [56, 57]. Warburg attributed aerobic glycolysis to mitochondrial dysfunction in cancer cells [58]. However, there is still no evidence to confirm this concept [59–61]. Mitophagy is an evolutionarily conserved cellular process that eliminates aged, dysfunctional, damaged or excessive mitochondria via selective autophagy. It has been documented that dysregulated mitophagy results in the accumulation of damaged mitochondria, and plays an important role in carcinogenesis and tumor progression [62]. In the p53-null radio-resistant cells, BNIP3-dependent clearance of abnormal mitochondria limits the glycolytic shift in head and neck squamous cell carcinoma [63], implying that mitophagy may regulate the metabolic switch to establish a balance between aerobic glycolysis and oxidative phosphorylation. Interestingly, vIRF1 activated NIX-mediated mitophagy to impair mitochondrial dynamics to increase KSHV replication [64]. Here, we demonstrated that vIRF1 induces aerobic glycolysis by degrading hnRNP Q1, however, the relationship between aerobic glycolysis and mitophagy in KSHV infection and lytic replication, and KS pathogenesis remains unclear.

hnRNP Q1 is not only highly expressed in colorectal cancer tissues [48], but also overexpressed in pancreatic cancer and associated with poor prognosis [65]. Moreover, loss of hnRNP Q1 promotes apoptosis of myeloid leukemia cells [66]. These studies show that hnRNP Q1 is potentially an oncogenic protein. However, the role of hnRNP Q1 in KSHV infection and KS pathogenesis is still not characterized. In the current study, we observed a lower level of hnRNP Q1 in KS lesion tissues, vIRF1-transduced endothelial cells and KSHV-infected endothelial cells. Mechanistically, vIRF1 upregulated and recruited E3 ubiquitin ligase KLHL3 to facilitate the formation of KLHL3/CUL3 ubiquitin ligase complex, resulting in hnRNP Q1 degradation. Overexpression of hnRNP Q1 inhibited vIRF1-induced aerobic glycolysis. Therefore, we revealed the importance of hnRNP Q1 in KSHV reprogramming of metabolism. It is worth noting that hnRNP Q1 might be growth-suppressive, which might be involved in KSHV infection and KS pathogenesis. The underlying mechanism requires further investigation.

Protein ubiquitination is one of the most extensively studied post-translational modifications that regulate protein functions by interfering with interaction with other proteins, altering cellular localization, and regulating stability. There are many types of ubiquitin linkages including K48, K63, K6, K11, K27, K29, and K33 [67]. Each type of polyubiquitin chain causes the diverse outcomes of ubiquitination. Here, we found vIRF1 mediated K48-ubiquitination of hnRNP Q1. In addition to K48-ubiquitination of hnRNP Q1, our results showed that vIRF1 might also regulate other forms of ubiquitination.

Furthermore, hnRNP Q1 is an RNA-binding protein primarily localized in the cytoplasm and participates in mRNA metabolism

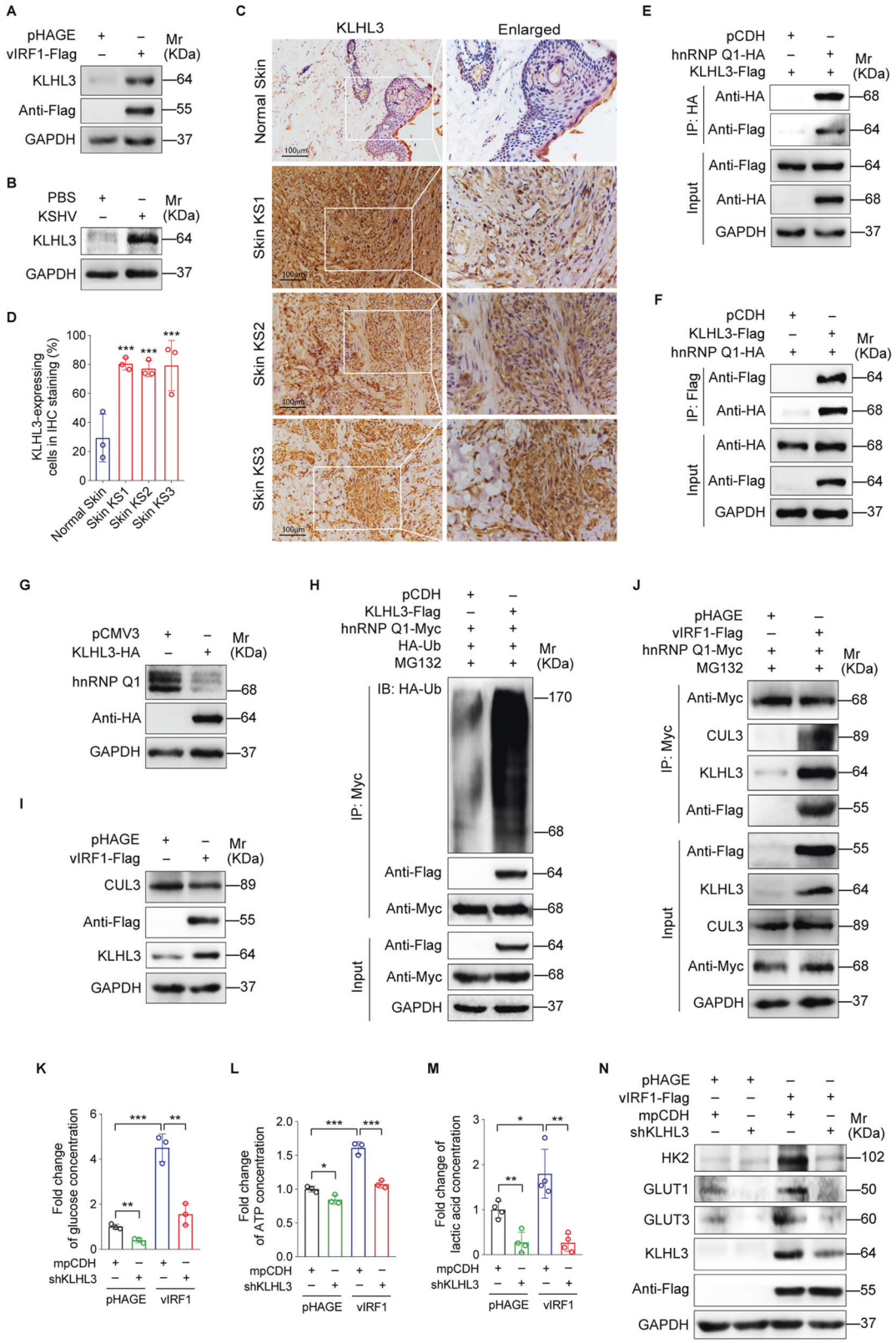

[45]. Here, we found that GDPD1 mRNA is a new hnRNP Q1 target. We confirmed the interaction between hnRNP Q1 and GDPD1 mRNA, and demonstrated that hnRNP Q1 increased GDPD1 mRNA stability. GDPD1, also called glycerophosphodiesterase 4, is a member of the glycerophosphodiester phosphodiesterase family of enzymes. A study suggests that GDPD1 is probably involved in bioactive N-acylethanolamine biosynthesis [68]. Currently, there is no report on the association of GDPD1 with viral infection and cancer. In this study, we detected a lower level of GDPD1 expression in vIRF1-transduced endothelial cells, KSHV-infected

Fig. 5 vIRF1 recruits the E3 ubiquitin ligase KLHL3 to degrade hnRNP Q1 and promote aerobic glycolysis. A Western blotting analysis of KLHL3 expression in endothelial cells transduced with 2 MOI lentiviral vIRF1 (**vIRF1**) or control lentivirus (**pHAGE**). **B** Western blotting analysis of KLHL3 expression in endothelial cells treated with PBS (**PBS**) or infected with wild type KSHV (**KSHV**). **C** H&E staining, and immunohistochemical staining of KLHL3 in normal skin, skin KS of patient #1 (**Skin KS1**), skin KS of patient #2 (**Skin KS2**), and skin KS of patient #3 (**Skin KS3**). Magnification, ×200, ×400. **D** Results were quantified in **C**. **E** KLHL3 overexpressed endothelial cells were transduced with lentiviral HA-tagged hnRNP Q1 or its control virus pCDH. The interaction between KLHL3 and hnRNP Q1 proteins was examined by immunoprecipitating with anti-HA antibody. **F** hnRNP Q1 overexpressed endothelial cells were transduced with lentiviral Flag-tagged KLHL3 or its control virus pCDH. The interaction between KLHL3 and hnRNP Q1 proteins was examined by immunoprecipitating with anti-Flag antibody. **G** Western blotting analysis of hnRNP Q1 expression in endothelial cells which were transfected with pCMV3-Flag-KLHL3 construct (**KLHL3**) or its control pCMV3-C-Flag (**pCMV**). **H** The HA-Ub and hnRNP Q1-Myc plasmids were co-transfected into endothelial cells. Cells were further transduced with lentiviral KLHL3-Flag or its control virus pCDH, and treated with MG132 (20 μM) for 6 h. Cells were subjected to immunoprecipitation assay (IP) with anti-Myc antibody for detection of hnRNP Q1 ubiquitination. **I** Western blotting analysis of CUL3 and KLHL3 expression in endothelial cells transduced with 2 MOI lentiviral vIRF1 (**vIRF1**) or control lentivirus (**pHAGE**). **J** hnRNP Q1 (hnRNP Q1-Myc) overexpressed endothelial cells were transduced with lentiviral vIRF1 and its control lentivirus pHAGE, and then further treated with MG132 (20 μM) for 6 h. Immunoprecipitation assay was performed to examine the interaction between hnRNP Q1 and KLHL3 /CUL3 complex with anti-Myc antibody. **K** Lentiviral vIRF1- or its control pHAGE-infected endothelial cells, followed by transduction with lentivirus expressing a mixture of shRNAs targeting KLHL3 (shKLHL3) were used to detect the levels of intracellular glucose. **L** Cells treated as in (**K**) were used to measure the levels of intracellular ATP. **M**. Cells treated as in (**K**) were used to measure lactate production. **N** Western blotting analysis of HK2, GLUT1 and GLUT3 expression in cells treated as in (**K**). Data were shown as mean ± SD. * $P < 0.05$, ** $P < 0.01$, and *** $P < 0.001$, Student's *t*-test.

endothelial cells compared to the controls, as well as in KS lesions compared to normal skin tissues. Notably, we observed that overexpression of GDPD1 suppressed vIRF1-induced aerobic glycolysis. This work is the first to report the role of GDPD1 in aerobic glycolysis and KS pathogenesis. However, how GDPD1 negatively regulates HK2, GLUT1 and GLUT3 to affect aerobic glycolysis, contributing to KSHV infection, replication and KS pathogenesis remains to be further explored.

In summary, we have revealed that vIRF1 is essential for KSHV-induced aerobic glycolysis during KSHV infection and replication. vIRF1 induces ubiquitination and degradation of hnRNP Q1 by recruiting KLHL3/CUL3 ubiquitin ligase complex. The reduction of hnRNP Q1 destabilizes GDPD1 mRNA (Fig. 8G) which enhances aerobic glycolysis. Our findings demonstrate a novel role of vIRF1 in regulating cellular metabolism and identify a potential new therapeutic target for KSHV infection and KSHV-induced cancers.

MATERIALS AND METHODS

Ethics statement

This study was reviewed and monitored by the Institutional Ethics Committee of the First Affiliated Hospital of Nanjing Medical University. A total of 3 pairs of KS patients' lesions and normal skin tissues were obtained and all patients were informed of the content of this study.

Cell culture and transfection

All of cell lines used in this study were authenticated by short tandem repeat profiling and routinely tested for mycoplasma using Myco-Blue Mycoplasma Detector (D103-01/02, Vazyme Biotech Co., Ltd, Nanjing, China). HEK293T and a human umbilical vein endothelial cell line EA.hy926 (catalog #CRL-2922TM; ATCC, Manassas, VA, USA) were cultured in Dulbecco's modified Eagle's medium (DMEM) containing 10% fetal bovine serum (FBS). iSLK-RGB-BAC16 and iSLK-RGB-K9 mutant cells were maintained in DMEM supplemented with 1.2 mg/ml hygromycin B, 250 μg/ml G418, 1 μg/ml puromycin, and 10% fetal bovine serum (FBS). HEK293T cells were transfected with Lipofectamine™ 2000 Reagent (Invitrogen, Carlsbad, CA, USA) and EA.hy926 was transfected with Effectence transfection reagent (Qiagen, Suzhou, Jiangsu, China).

Reagents and plasmids

MG132, a proteasome inhibitor, was obtained from Selleck Chemicals (Shanghai, China). Cycloheximide (CHX) was from Cell Signal Technology. Actinomycin D was from Sigma-Aldrich. The expressing plasmids of vIRF1-Flag were generated as previously described [35]. The skeleton plasmid of lentiviral vectors hnRNP Q1-Myc, hnRNP Q1-HA, KLHL3-Flag and GDPD1-Flag was pCDH-CMV-MCS-EF1-copGFP (pCDH for short). The short hairpin RNA sequences (shRNAs) targeting KLHL3 and hnRNP Q1 are listed in Supplementary Table 1. The control vector of all the shRNAs was constructed in our previous study [69]. pCMV3-HA-KLHL3 construct containing KLHL3 cDNA was purchased from Sino Biological Inc. (Beijing, China). All constructs were confirmed by DNA sequencing.

Lentivirus packaging and infection

Lentiviruses were generated by co-transfecting HEK293T cells with the packaging plasmid, psPAX2, the envelope plasmid, pMD2.G, and the lentivirus plasmid, pHAGE, which has a GFP cassette as previously described [70, 71].

qRT-PCR analysis

Total RNA was extracted with TRIzol (Life Technologies, Grand Island, NY, USA). After preparing the cDNA using HiScript Q RT SuperMix (Vazyme Biotech Co., Ltd, Nanjing, China), the quantitative real-time PCR (qRT-PCR) analysis was performed using AceQ qPCR SYBR Green Master Mix (Vazyme Biotech Co., Ltd, Nanjing, China) on Applied Biosystems (ABI, Foster City, CA, USA). The primer sequences for qRT-PCR used in this study are summarized in Supplementary Table 2. Data were normalized by the level of GAPDH expression in each sample.

Western blotting and antibodies

Levels of protein expression were analyzed by Western blotting as described previously [69, 72]. Anti-HK2 rabbit antibody, anti-GLUT1 rabbit antibody, anti-GAPDH mouse antibody, and anti-hnRNP Q1 mouse antibody were obtained from Santa Cruz Biotechnology (Dallas, TX, USA). Anti-Flag mouse antibody, anti-HA mouse antibody, and anti-Myc mouse antibody were from MEDICAL & BIOLOGICAL LABORATORIES CO., LTD. (Seoul, Korea). Anti-GLUT3 rabbit antibody, anti-KLHL3 rabbit antibody and anti-GDPD1 rabbit antibody were purchased from Proteintech Group, Inc. (Wuhan, China). Anti-CUL3 rabbit antibody was from Abcam (Cambridge, MA, USA). Anti-GST rabbit antibody and anti-His mouse antibody were from Beyotime Institute of Biotechnology (Nantong, Jiangsu, China). The full length original Western blots are provided in Supplementary File 1

Immunohistochemistry (IHC) staining

For immunohistochemistry (IHC) staining, all formalin-fixed and paraffin-embedded (FFPE) samples were immunostained with the indicated antibodies following standard methodology. Antibodies used for IHC were anti-KSHV LANA rat antibody from Advanced Biotechnologies Inc. (Columbia, MD, USA), anti-hnRNP Q1 rabbit from ABclonal Technology Co.,Ltd. (Wuhan, China), anti-KLHL3 rabbit antibody and anti-GDPD1 rabbit antibody from Proteintech Group, Inc. (Wuhan, China). Horseradish peroxidase (HRP)-labeled goat anti-rat or anti-rabbit (Beyotime Institute of Biotechnology, Nantong, Jiangsu, China) were used as secondary antibodies. DAB (3,3′-diaminobenzidine) Peroxidase (HRP) Substrate Kit (VECTOR LABORATORIES, INC., Burlingame, USA) was used to visualize staining. For quantification of immunohistochemistry staining, we selected three fields randomly of each sample and photographed the images of 200x and 400x magnification, respectively. All the cells in the images of 400x magnification were counted to calculate the percentage of positive cells by a pathologist with a double-blinded randomized control design. The representative images were taken from three randomly selected fields of each sample.

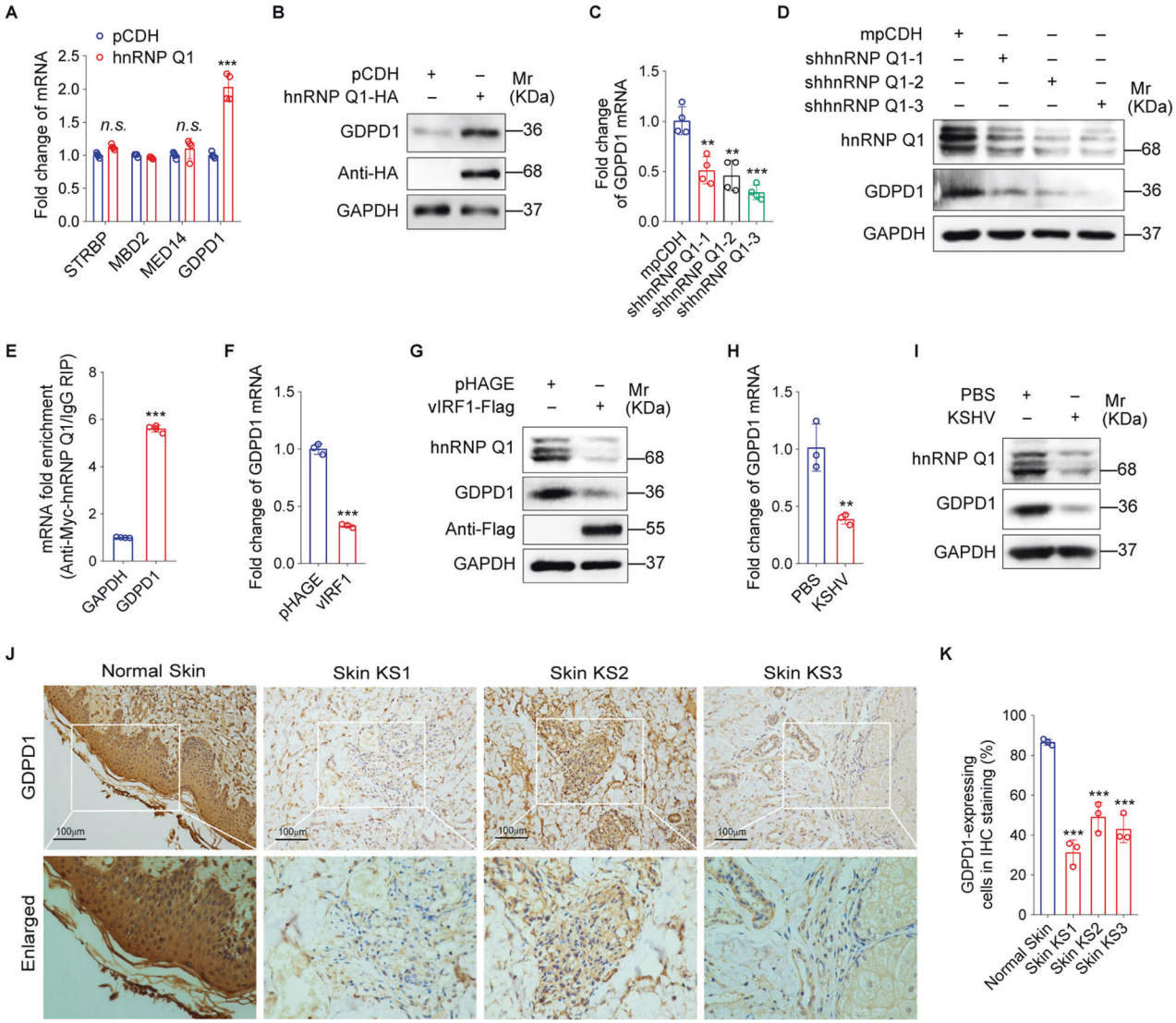

Fig. 6 GDPD1 mRNA is the target of hnRNP Q1. A qRT-PCR analysis of STRBP, MBD2, MED14 and GDPD1 mRNA levels in endothelial cells transduced with lentiviral hnRNP Q1 (**hnRNP Q1**) and its control lentivirus (**pCDH**). **B** Western blotting analysis of GDPD1 protein level in cells treated as in (**A**). **C** qRT-PCR analysis of GDPD1 mRNA level in endothelial cells transduced with lentivirus-mediated No.1 (shhnRNP Q1-1), No.2 (shhnRNP Q1-2) and No. 3 (shhnRNP Q1-3) shRNAs targeting hnRNP Q1. **D** Western blotting analysis of GDPD1 expression in cells treated as in (**C**). **E** RNA immunoprecipitation analysis of the interaction between hnRNP Q1 and GDPD1 mRNA with anti-Myc antibody. GAPDH was used as a control. **F** qRT-PCR analysis of GDPD1 mRNA level in endothelial cells transduced with 2 MOI lentiviral vIRF1 (**vIRF1**) or control lentivirus (**pHAGE**). **G** Western blotting analysis of GDPD1 expression in endothelial cells transduced with 2 MOI lentiviral vIRF1 (**vIRF1**) or control lentivirus (**pHAGE**). **H** qRT-PCR analysis of GDPD1 mRNA level in endothelial cells treated with PBS (**PBS**) or infected with wild type KSHV (**KSHV**). **I** Western blotting analysis of GDPD1 expression in endothelial cells treated with PBS (**PBS**) or infected with wild type KSHV (**KSHV**). **J** H&E staining, and immunohistochemical staining of GDPD1 protein in normal skin, skin KS of patient #1 (**Skin KS1**), skin KS of patient #2 (**Skin KS2**), and skin KS of patient #3 (**Skin KS3**). Magnification, ×200, ×400. **K** Results were quantified in **J** Data were shown as mean ± SD. $^{**}P < 0.01$, and $^{***}P < 0.001$, Student's *t*-test. *n.s.*, not significant.

Glucose uptake and lactate production assay

Cells were cultured in glucose-free DMEM for 8 h, and then replaced the culture and incubated with high-glucose DMEM for an additional 24 h. Cells were harvested for detection of the levels of intracellular glucose using a fluorescence-based glucoseassay kit (BioVision) according to manufacturer's instructions as described previously [73, 74]. The culture medium was harvested for detection of lactate levels in the culture medium using the Lactate Assay Kit (Jiancheng BioEngineering, Nanjing, China) according to the manufacturer's instructions.

ATP assessment

ATP production was measured using the ATP Assay Kit (Beyotime Institute of Biotechnology, Nantong, Jiangsu, China) according to the manufacturer's instructions. Cells were collected, washed and then ultrasonicated. After centrifuged, the supernatant was transferred for ATP test at 562 nm with Bicinchoninic Acid assay.

Immunofluorescence assay (IFA)

To detect the colocalization of vIRF1 and hnRNP Q1, hnRNP Q1-overexpressing cells were transfected with vIRF1-Flag construct or its control construct, and then were seeded on 12 mm diameter round glass coverslips in 24-well plates. After incubation overnight for attachment, cells were fixed in cold acetone for 15 min, permeabilized with 0.2% Triton X-100 for 15 min, blocked with 1% bovine serum albumin for 1 h, and then were incubated with primary antibodies against Myc mouse (1:200 dilution) and Flag rabbit (1:200 dilution) at 4 °C overnight. Alexa Fluor 488-coupled anti-rabbit and Alexa Fluor 555-coupled anti-mouse secondary antibodies (Beyotime Institute of Biotechnology, Nantong, China) were

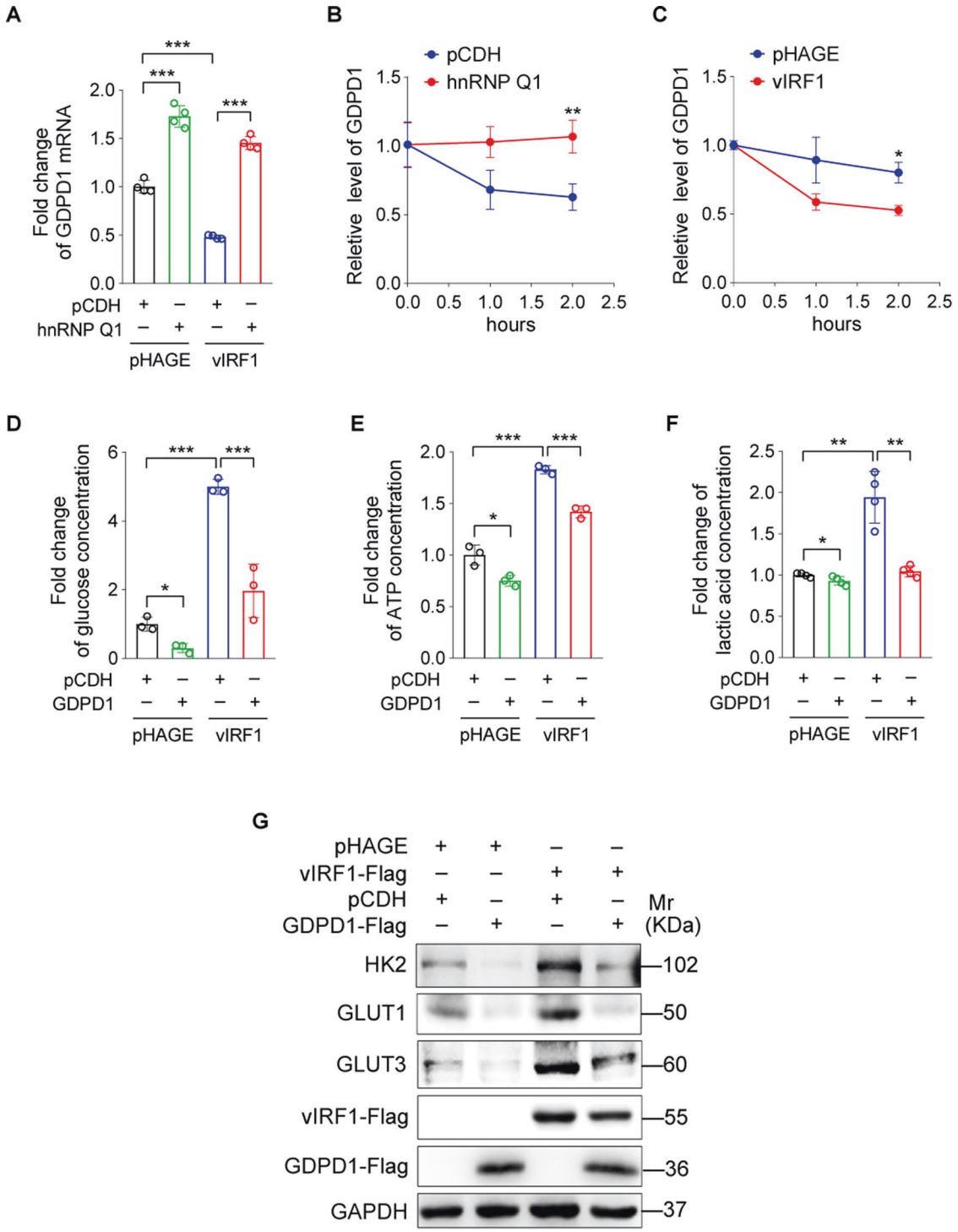

Fig. 7 vIRF1-downregulated hnRNP Q1 reduces the stability of GDPD1 mRNA to induce aerobic glycolysis. A Lentiviral vIRF1- or its control pHAGE-infected endothelial cells were transduced with lentiviral hnRNP Q1 and its control lentivirus pCDH. Cells were collected for qRT-PCR analysis of GDPD1 mRNA level. **B** Endothelial cells transduced with lentiviral hnRNP Q1 or control lentivirus pCDH were treated with actinomycin D. RNA decay assays were performed to examine the degradation rate of GDPD1 mRNA. **C** Endothelial cells transduced with 2 MOI lentiviral vIRF1 (**vIRF1**) or control lentivirus (**pHAGE**) were treated with actinomycin D. RNA decay assays were performed to detect the degradation rate of GDPD1 mRNA. **D** Lentiviral vIRF1- or its control pHAGE-infected endothelial cells were transduced by lentiviral GDPD1 (**GDPD1-Flag**) and control lentivirus (**pCDH**). Cells were used to detect the level of intracellular glucose. **E** Cells treated as in (**D**) were used to measure the levels of intracellular ATP. **F** Cells treated as in (**D**) were used to measure lactate production. **G** Western blotting analysis of HK2, GLUT1 and GLUT3 expression in cells treated as in (**D**). Data were shown as mean ± SD. *$P < 0.05$, **$P < 0.01$, and ***$P < 0.001$, Student's *t*-test.

incubated for 1 h. After incubation with 4, 6 diamidino-2-phenylindole (DAPI) (Beyotime Institute of Biotechnology, Nantong, Jiangsu, China) for 10 min, images were acquired using a Carl Zeiss LSM710 confocal microscopy (Carl Zeiss, Freistaat Thü ringen, Germany).

RNA immunoprecipitation (RIP)

RIP experiments were performed using the Magna RIP RNA-Binding Protein Immunoprecipitation kit (Millipore, 17–700). The whole cell lysates were incubated with protein A + G magnetic beads conjugated using 5 μg of

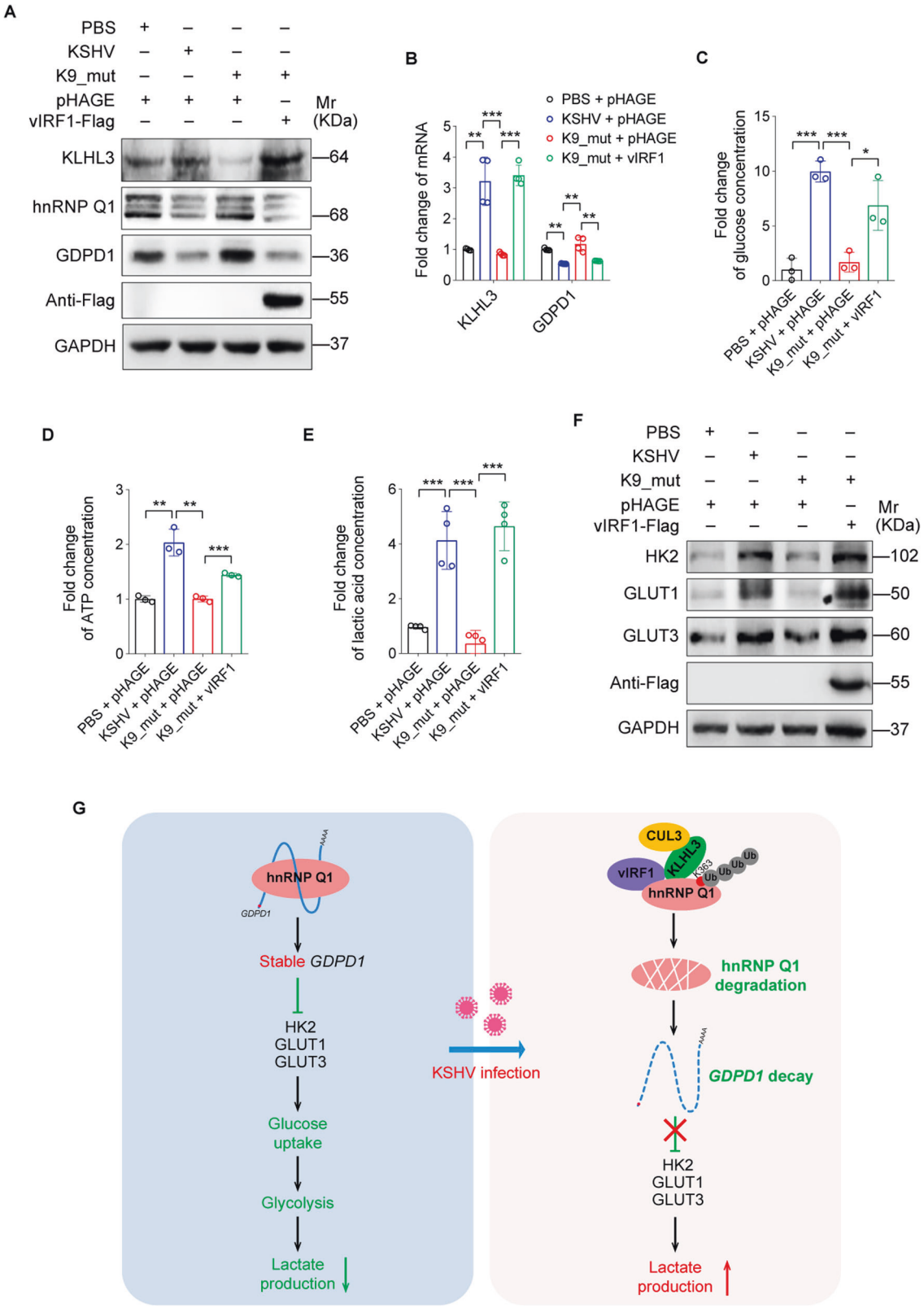

Fig. 8 Loss of vIRF1 reduces KSHV-induced aerobic glycolysis. A Western blotting analysis of KLHL3, hnRNP Q1 and GDPD1 expression in endothelial cells treated with PBS (**PBS**), infected with wild-type KSHV (**KSHV**) or K9 mutant virus (**K9_mut**) followed by transduction with lentiviral vIRF1. **B** qRT-PCR analysis of KLHL3 and GDPD1 mRNA levels in cells treated as in (**A**). **C** Cells treated as in (**A**) were used to examine the level of intracellular glucose. **D** Cells treated as in (**A**) were used to measure the level of intracellular ATP. **E** Cells treated as in (**A**) were used to detect lactate production. **F** Western blotting analysis of HK2, GLUT1 and GLUT3 expression in cells treated as in (**A**). **G** Schematic illustration for the mechanism of vIRF1-induced aerobic glycolysis. KSHV vIRF1 recruits E3 ubiquitin ligase complex KLHL3/CUL3 to degrade RNA-binding protein hnRNP Q1. The downregulated hnRNP Q1 accelerates GDPD1 mRNA decay to increase glucose uptake, and lactate secretion. Data were shown as mean ± SD. $^{*}P < 0.05$, $^{**}P < 0.01$, and $^{***}P < 0.001$, Student's *t*-test.

Myc-tag antibodies (MEDICAL & BIOLOGICAL LABORATORIES CO., LTD.) or control IgG at 4 °C for overnight. The immunoprecipitated RNA was purified and detected by qRT-PCR. The sequences of specific primers for RIP-qPCR are listed in Supplementary Table 3.

Co-immunoprecipitation and GST pulldown

Co-immunoprecipitation and GST pulldown were performed as previously described [75]. For co-IP, the IPKine™ HRP goat anti-mouse or anti-rabbit IgG LCS (Abbkine Scientific Co., Ltd. Wuhan, China) were used to avoid the detection of the heavy chains of IgG. For GST pulldown, the GST-vIRF1 plasmid was constructed by inserting the full-length vIRF1 open reading frame into pGEX-4T-3 (GE Healthcare, Piscataway, USA). Plasmid expressing hnRNP Q1 fusion protein was constructed in the pET32a (+) vector (EMD Chemicals, CA, USA).

Statistical analysis

All experiments were performed at least three times, unless otherwise stated. Results are presented as the means ± SD. Sample sizes for relevant experiments were determined by power analyses conducted during experiment planning. Statistical analysis was based on chi-square test for Figs. 1D, 5D and 6K. The remaining statistical comparisons were carried out using Student's *t-test* for statistical analysis of two groups. Differences with a P value of 0.05 or less were considered significant.

DATA AVAILABILITY

Data supporting the present study are available from the corresponding author upon reasonable request.

REFERENCES

1. Bannai H, Fukatsu K, Mizutani A, Natsume T, Iemura S, Ikegami T, et al. An RNA-interacting protein, SYNCRIP (heterogeneous nuclear ribonuclear protein Q1/NSAP1) is a component of mRNA granule transported with inositol 1,4,5-trisphosphate receptor type 1 mRNA in neuronal dendrites. J Biol Chem. 2004;279:53427–34.
2. Cesarman E, Damania B, Krown SE, Martin J, Bower M, Whitby D. Kaposi sarcoma. Nat Rev Dis Prim. 2019;5:9.
3. Bhutani M, Polizzotto MN, Uldrick TS, Yarchoan R. Kaposi sarcoma-associated herpesvirus-associated malignancies: epidemiology, pathogenesis, and advances in treatment. Semin Oncol. 2015;42:223–46.
4. Soulier J, Grollet L, Oksenhendler E, Cacoub P, Cazals-Hatem D, Babinet P, et al. Kaposi's sarcoma-associated herpesvirus-like DNA sequences in multicentric Castleman's disease. Blood. 1995;86:1276–80.
5. Warburg O, Wind F, Negelein E. The metabolism of tumors in the body. J Gen Physiol. 1927;8:519–30.
6. Liberti MV, Locasale JW. The Warburg effect: how does it benefit cancer cells? Trends Biochem Sci. 2016;41:211–8.
7. Hsu PP, Sabatini DM. Cancer cell metabolism: Warburg and beyond. Cell. 2008;134:703–7.
8. Vander Heiden MG, Cantley LC, Thompson CB. Understanding the Warburg effect: the metabolic requirements of cell proliferation. Science. 2009;324:1029–33.
9. Purdy JG, Luftig MA. Reprogramming of cellular metabolic pathways by human oncogenic viruses. Curr Opin Virol. 2019;39:60–69.
10. Yu L, Chen X, Wang L, Chen S. Oncogenic virus-induced aerobic glycolysis and tumorigenesis. J Cancer. 2018;9:3699–706.
11. Icard P, Lincet H, Wu Z, Coquerel A, Forgez P, Alifano M, et al. The key role of Warburg effect in SARS-CoV-2 replication and associated inflammatory response. Biochimie. 2021;180:169–77.
12. Wu YH, Yang Y, Chen CH, Hsiao CJ, Li TN, Liao KJ, et al. Aerobic glycolysis supports hepatitis B virus protein synthesis through interaction between viral surface antigen and pyruvate kinase isoform M2. PLoS Pathog. 2021;17:e1008866.
13. Prusinkiewicz MA, Tu J, Dodge MJ, MacNeil KM, Radko-Juettner S, Fonseca GJ, et al. Differential effects of human Adenovirus E1A protein isoforms on aerobic Glycolysis in A549 human lung epithelial cells. Viruses 2020;12:610.
14. Guo X, Wu S, Li N, Lin Q, Liu L, Liang H, et al. Accelerated metabolite levels of aerobic glycolysis and the pentose phosphate pathway are required for efficient replication of infectious spleen and kidney necrosis virus in chinese perch brain cells. *Biomolecules* 2019;9:440.
15. Lyu X, Wang J, Guo X, Wu G, Jiao Y, Faleti OD, et al. EBV-miR-BART1-5P activates AMPK/mTOR/HIF1 pathway via a PTEN independent manner to promote glycolysis and angiogenesis in nasopharyngeal carcinoma. PLoS Pathog. 2018;14:e1007484.
16. Mushtaq M, Darekar S, Kashuba E. DNA tumor viruses and cell metabolism. Oxid Med Cell Longev. 2016;2016:6468342.
17. Ye F, Lei X, Gao SJ, Mechanisms of Kaposi's Sarcoma-associated herpesvirus latency and reactivation. Adv Virol. 2011:2011:193860.
18. Delgado T, Carroll PA, Punjabi AS, Margineantu D, Hockenbery DM, Lagunoff M. Induction of the Warburg effect by Kaposi's sarcoma herpesvirus is required for the maintenance of latently infected endothelial cells. Proc Natl Acad Sci USA. 2010;107:10696–701.
19. Delgado T, Sanchez EL, Camarda R, Lagunoff M. Global metabolic profiling of infection by an oncogenic virus: KSHV induces and requires lipogenesis for survival of latent infection. PLoS Pathog. 2012;8:e1002866.
20. Ma T, Patel H, Babapoor-Farrokhran S, Franklin R, Semenza GL, Sodhi A, et al. KSHV induces aerobic glycolysis and angiogenesis through HIF-1-dependent upregulation of pyruvate kinase 2 in Kaposi's sarcoma. Angiogenesis. 2015;18:477–88.
21. Yogev O, Lagos D, Enver T, Boshoff C. Kaposi's sarcoma herpesvirus microRNAs induce metabolic transformation of infected cells. PLoS Pathog. 2014;10:e1004400.
22. Karki R, Lang SM, Means RE. The MARCH family E3 ubiquitin ligase K5 alters monocyte metabolism and proliferation through receptor tyrosine kinase modulation. PLoS Pathog. 2011;7:e1001331.
23. Cai Q, Lan K, Verma SC, Si H, Lin D, Robertson ES. Kaposi's sarcoma-associated herpesvirus latent protein LANA interacts with HIF-1 alpha to upregulate RTA expression during hypoxia: Latency control under low oxygen conditions. J Virol. 2006;80:7965–75.
24. Zhu Y, Ramos da Silva S, He M, Liang Q, Lu C, Feng P, et al. An Oncogenic Virus Promotes Cell Survival and Cellular Transformation by Suppressing Glycolysis. PLoS Pathog. 2016;12:e1005648.
25. Zhu Y, Li T, Ramos da Silva S, Lee JJ, Lu C, Eoh H, et al. A critical role of glutamine and asparagine gamma-nitrogen in nucleotide biosynthesis in cancer cells hijacked by an oncogenic virus. *mBio* 2017;8:e01179-17.
26. Li T, Zhu Y, Cheng F, Lu C, Jung JU, Gao SJ, Oncogenic Kaposi's Sarcoma-Associated Herpesvirus Upregulates Argininosuccinate Synthase 1, a rate-limiting enzyme of the citrulline-nitric oxide cycle, to activate the STAT3 pathway and promote growth transformation. *J Virol.* 2019;93:e01599-18.
27. Li T, Gao SJ. Metabolic reprogramming and metabolic sensors in KSHV-induced cancers and KSHV infection. Cell Biosci. 2021;11:176.
28. Hew K, Dahlroth SL, Venkatachalam R, Nasertorabi F, Lim BT, Cornvik T, et al. The crystal structure of the DNA-binding domain of vIRF-1 from the oncogenic KSHV reveals a conserved fold for DNA binding and reinforces its role as a transcription factor. Nucleic Acids Res. 2013;41:4295–306.
29. Gao SJ, Boshoff C, Jayachandra S, Weiss RA, Chang Y, Moore PS. KSHV ORF K9 (vIRF) is an oncogene which inhibits the interferon signaling pathway. Oncogene. 1997;15:1979–85.
30. Kirchhoff S, Sebens T, Baumann S, Krueger A, Zawatzky R, Li-Weber M, et al. Viral IFN-regulatory factors inhibit activation-induced cell death via two positive regulatory IFN-regulatory factor 1-dependent domains in the CD95 ligand promoter. J Immunol. 2002;168:1226–34.
31. Seo T, Park J, Choe J. Kaposi's sarcoma-associated herpesvirus viral IFN regulatory factor 1 inhibits transforming growth factor-beta signaling. Cancer Res. 2005;65:1738–47.
32. Seo T, Park J, Lee D, Hwang SG, Choe J. Viral interferon regulatory factor 1 of Kaposi's sarcoma-associated herpesvirus binds to p53 and represses p53-dependent transcription and apoptosis. J Virol. 2001;75:6193–8.
33. Nakamura H, Li M, Zarycki J, Jung JU. Inhibition of p53 tumor suppressor by viral interferon regulatory factor. J Virol. 2001;75:7572–82.
34. Shin YC, Nakamura H, Liang X, Feng P, Chang H, Kowalik TF, et al. Inhibition of the ATM/p53 signal transduction pathway by Kaposi's sarcoma-associated herpesvirus interferon regulatory factor 1. J Virol. 2006;80:2257–66.
35. Li W, Wang Q, Feng Q, Wang F, Yan Q, Gao SJ, et al. Oncogenic KSHV-encoded interferon regulatory factor upregulates HMGB2 and CMPK1 expression to promote cell invasion by disrupting a complex lncRNA-OIP5-AS1/miR-218-5p network. PLoS Pathog. 2019;15:e1007578.
36. Li W, Wang Q, Qi X, Lu H, Chen Y, Shi J, et al. An oncogenic viral interferon regulatory factor upregulates CUB domain-containing protein 1 to promote angiogenesis by hijacking transcription factor lymphoid enhancer-binding factor 1 and metastasis suppressor CD82. Cell Death Differ. 2020;27:3289–306.
37. Li W, Wang F, Shi J, Feng Q, Chen Y, Qi X, et al. Sperm associated antigen 9 promotes oncogenic KSHV-encoded interferon regulatory factor-induced cellular transformation and angiogenesis by activating the JNK/VEGFA pathway. PLoS Pathog. 2020;16:e1008730.
38. Yao S, Jia X, Wang F, Sheng L, Song P, Cao Y, et al. CircRNA ARFGEF1 functions as a ceRNA to promote oncogenic KSHV-encoded viral interferon regulatory factor induction of cell invasion and angiogenesis by upregulating glutaredoxin 3. PLoS Pathog. 2021;17:e1009294.

39. Mizutani A, Fukuda M, Ibata K, Shiraishi Y, Mikoshiba K. SYNCRIP, a cytoplasmic counterpart of heterogeneous nuclear ribonucleoprotein R, interacts with ubiquitous synaptotagmin isoforms. J Biol Chem. 2000;275:9823–31.
40. Rossoll W, Kroning AK, Ohndorf UM, Steegborn C, Jablonka S, Sendtner M. Specific interaction of Smn, the spinal muscular atrophy determining gene product, with hnRNP-R and gry-rbp/hnRNP-Q: a role for Smn in RNA processing in motor axons? Hum Mol Genet. 2002;11:93–105.
41. Mourelatos Z, Abel L, Yong J, Kataoka N, Dreyfuss G. SMN interacts with a novel family of hnRNP and spliceosomal proteins. EMBO J. 2001;20:5443–52.
42. Blanc V, Navaratnam N, Henderson JO, Anant S, Kennedy S, Jarmuz A, et al. Identification of GRY-RBP as an apolipoprotein B RNA-binding protein that interacts with both apobec-1 and apobec-1 complementation factor to modulate C to U editing. J Biol Chem. 2001;276:10272–83.
43. Chen HH, Chang JG, Lu RM, Peng TY, Tarn WY. The RNA binding protein hnRNP Q modulates the utilization of exon 7 in the survival motor neuron 2 (SMN2) gene. Mol Cell Biol. 2008;28:6929–38.
44. Kim DY, Woo KC, Lee KH, Kim TD, Kim KT, hnRNP Q. and PTB modulate the circadian oscillation of mouse Rev-erb alpha via IRES-mediated translation. Nucleic Acids Res. 2010;38:7068–78.
45. Weidensdorfer D, Stohr N, Baude A, Lederer M, Kohn M, Schierhorn A, et al. Control of c-myc mRNA stability by IGF2BP1-associated cytoplasmic RNPs. RNA. 2009;15:104–15.
46. Chen HH, Yu HI, Chiang WC, Lin YD, Shia BC, Tarn WY. hnRNP Q regulates Cdc42-mediated neuronal morphogenesis. Mol Cell Biol. 2012;32:2224–38.
47. Lai CH, Huang YC, Lee JC, Tseng JT, Chang KC, Chen YJ, et al. Translational upregulation of Aurora-A by hnRNP Q1 contributes to cell proliferation and tumorigenesis in colorectal cancer. Cell Death Dis. 2017;8:e2555.
48. Wang YC, Chang KC, Lin BW, Lee JC, Lai CH, Lin LJ, et al. The EGF/hnRNP Q1 axis is involved in tumorigenesis via the regulation of cell cycle-related genes. Exp Mol Med. 2018;50:1–14.
49. Lagunoff M. Activation of cellular metabolism during latent Kaposi's Sarcoma herpesvirus infection. Curr Opin Virol. 2016;19:45–49.
50. Sohara E, Uchida S. Kelch-like 3/Cullin 3 ubiquitin ligase complex and WNK signaling in salt-sensitive hypertension and electrolyte disorder. Nephrol Dial Transpl. 2016;31:1417–24.
51. Koppenol WH, Bounds PL, Dang CV. Otto Warburg's contributions to current concepts of cancer metabolism. Nat Rev Cancer. 2011;11:325–37.
52. Locasale JW. The consequences of enhanced cell-autonomous glucose metabolism. Trends Endocrinol Metab. 2012;23:545–51.
53. Lunt SY, Vander, Heiden MG. Aerobic glycolysis: meeting the metabolic requirements of cell proliferation. Annu Rev Cell Dev Biol. 2011;27:441–64.
54. Liu X, Zhu C, Wang Y, Wei F, Cai Q. KSHV reprogramming of host energy metabolism for pathogenesis. Front Cell Infect Microbiol. 2021;11:621156.
55. Singh RK, Lang F, Pei Y, Jha HC, Robertson ES. Metabolic reprogramming of Kaposi's sarcoma associated herpes virus infected B-cells in hypoxia. PLoS Pathog. 2018;14:e1007062.
56. Rodriguez-Enriquez S, Moreno-Sanchez R. Intermediary metabolism of fast-growth tumor cells. Arch Med Res. 1998;29:1–12.
57. Vaupel P, Okunieff P, Neuringer LJ. Blood flow, tissue oxygenation, pH distribution, and energy metabolism of murine mammary adenocarcinomas during growth. Adv Exp Med Biol. 1989;248:835–45.
58. Warburg O. On the origin of cancer cells. Science. 1956;123:309–14.
59. Eakin RT, Morgan LO, Gregg CT, Matwiyoff NA. Carbon-13 nuclear magnetic resonance spectroscopy of living cells and their metabolism of a specifically labeled 13C substrate. FEBS Lett. 1972;28:259–64.
60. Fantin VR, Leder P. Mitochondriotoxic compounds for cancer therapy. Oncogene. 2006;25:4787–97.
61. Moreno-Sanchez R, Rodriguez-Enriquez S, Marin-Hernandez A, Saavedra E. Energy metabolism in tumor cells. FEBS J. 2007;274:1393–418.
62. Panigrahi DP, Praharaj PP, Bhol CS, Mahapatra KK, Patra S, Behera BP, et al. The emerging, multifaceted role of mitophagy in cancer and cancer therapeutics. Semin Cancer Biol. 2020;66:45–58.
63. Chang HW, Kim MR, Lee HJ, Lee HM, Kim GC, Lee YS, et al. p53/BNIP3-dependent mitophagy limits glycolytic shift in radioresistant cancer. Oncogene. 2019;38:3729–42.
64. Vo MT, Smith BJ, Nicholas J, Choi YB. Activation of NIX-mediated mitophagy by an interferon regulatory factor homologue of human herpesvirus. Nat Commun. 2019;10:3203.
65. Zhang P, Cao M, Zhang Y, Xu L, Meng F, Wu X, et al. A novel antisense lncRNA NT5E promotes progression by modulating the expression of SYNCRIP and predicts a poor prognosis in pancreatic cancer. J Cell Mol Med. 2020;24:10898–912.
66. Vu LP, Prieto C, Amin EM, Chhangawala S, Krivtsov A, Calvo-Vidal MN, et al. Functional screen of MSI2 interactors identifies an essential role for SYNCRIP in myeloid leukemia stem cells. Nat Genet. 2017;49:866–75.
67. Tracz M, Bialek W. Beyond K48 and K63: non-canonical protein ubiquitination. Cell Mol Biol Lett. 2021;26:1.
68. Tsuboi K, Okamoto Y, Rahman IA, Uyama T, Inoue T, Tokumura A, et al. Glycerophosphodiesterase GDE4 as a novel lysophospholipase D: a possible involvement in bioactive N-acylethanolamine biosynthesis. Biochim Biophys Acta. 2015;1851:537–48.
69. Hu M, Wang C, Li W, Lu W, Bai Z, Qin D, et al. A KSHV microRNA directly targets G protein-coupled Receptor Kinase 2 to promote the migration and invasion of endothelial cells by inducing CXCR2 and activating AKT signaling. PLoS Pathog. 2015;11:e1005171.
70. Xue M, Yao S, Hu M, Li W, Hao T, Zhou F, et al. HIV-1 Nef and KSHV oncogene K1 synergistically promote angiogenesis by inducing cellular miR-718 to regulate the PTEN/AKT/mTOR signaling pathway. Nucleic Acids Res. 2014;42:9862–79.
71. Yao S, Hu M, Hao T, Li W, Xue X, Xue M, et al. MiRNA-891a-5p mediates HIV-1 Tat and KSHV Orf-K1 synergistic induction of angiogenesis by activating NF-kappaB signaling. Nucleic Acids Res. 2015;43:9362–78.
72. Ding X, Xu J, Wang C, Feng Q, Wang Q, Yang Y, et al. Suppression of the SAP18/HDAC1 complex by targeting TRIM56 and Nanog is essential for oncogenic viral FLICE-inhibitory protein-induced acetylation of p65/RelA, NF-kappaB activation, and promotion of cell invasion and angiogenesis. Cell Death Differ. 2019;26:1970–86.
73. Xiang S, Gu H, Jin L, Thorne RF, Zhang XD, Wu M. LncRNA IDH1-AS1 links the functions of c-Myc and HIF1alpha via IDH1 to regulate the Warburg effect. Proc Natl Acad Sci USA. 2018;115:E1465–E1474.
74. Li L, Ma Y, Maerkeya K, Reyanguly D, Han L. LncRNA OIP5-AS1 regulates the Warburg effect through miR-124-5p/IDH2/HIF-1alpha pathway in cervical cancer. Front Cell Dev Biol. 2021;9:655018.
75. Li W, Yan Q, Ding X, Shen C, Hu M, Zhu Y, et al. The SH3BGR/STAT3 pathway regulates cell migration and angiogenesis induced by a gammaherpesvirus MicroRNA. PLoS Pathog. 2016;12:e1005605.

ACKNOWLEDGEMENTS

We are grateful to members from Dr. Lu laboratory for performing some preliminary experiments and providing useful information and helpful discussion. We thank Drs. Gary Hayward from Viral Oncology Program, The Johns Hopkins School of Medicine, and Young Bong Choi from Johns Hopkins University School of Medicine for providing the polyclonal rabbit anti-vIRF1 antibody and information related to source of vIRF1 antibody, respectively. This work was supported by grants from National Natural Science Foundation of China (81730062, 81761128003, 82072275, 31800148, 82172262, 81871642, 32170151, and 81902639), grants from Natural Science Foundation of Jiangsu Province (BK20180681 and BK20180084), grants from China Postdoctoral Science Foundation (2019TQ0158 and 2019M661889), and a grant from NIH (R01CA213275).

AUTHOR CONTRIBUTIONS

X.Q., Y.S. and R.Z. performed the experiments; W. L. and X. D. drew the pattern diagram; Q. Y., W.L. and C.L. conceived the experiments; X. D., Q.Y., W. L. and C.L. obtained funding for this work; W.L. wrote the draft of manuscript; W.L., S.J.G., and C.L. reviewed and edited the manuscript.

COMPETING INTERESTS

The authors declare no competing interests.

ADDITIONAL INFORMATION

Supplementary information The online version contains supplementary material available at https://doi.org/10.1038/s41418-022-01011-1.

Correspondence and requests for materials should be addressed to Wan Li or Chun Lu.